

# Point-contact spectroscopy of the antiferromagnetic superconductor $\text{HoNi}_2\text{B}_2\text{C}$ in the normal and superconducting state

Yu.G. Naidyuk, O.E. Kvitnitskaya, I.K. Yanson

*B. Verkin Institute for Low Temperature Physics and Engineering,  
National Academy of Sciences of Ukraine, 47 Lenin Ave., 61103, Kharkiv, Ukraine*

G. Fuchs, K. Nenkov, A. Wälte, G. Behr, D. Souptel, and S.-L. Drechsler

*Leibniz-Institut für Festkörper- und Werkstoffforschung Dresden e.V., Postfach 270116, D-01069 Dresden, Germany*

(Dated: October 29, 2018)

Point-contact (PC) spectroscopy measurements on antiferromagnetic (AF) ( $T_N \simeq 5.2$  K)  $\text{HoNi}_2\text{B}_2\text{C}$  single crystals in the normal and two different superconducting (SC) states ( $T_c \simeq 8.5$  K and  $T_c^* \simeq 5.6$  K) are reported. The PC study of the electron-boson(phonon) interaction (EB(P)I) spectral function reveals pronounced phonon maxima at 16, 22 and 34 meV. For the first time the high energy maxima at about 50 meV and 100 meV are resolved. Additionally, an admixture of a crystalline-electric-field (CEF) excitations with a maximum near 10 meV and a ‘magnetic’ peak near 3 meV are observed. The contribution of the 10-meV peak in PC EPI constant  $\lambda_{\text{PC}}$  is evaluated as 20-30%, while contribution of the high energy modes at 50 and 100 meV amounts about 10% for each maxima, so the superconductivity might be affected by CEF excitations. The SC gap in  $\text{HoNi}_2\text{B}_2\text{C}$  exhibits a standard single-band BCS-like dependence, but vanishes at  $T_c^* \simeq 5.6$  K  $< T_c$ , with  $2\Delta/k_B T_c^* \simeq 3.9$ . The strong coupling Eliashberg analysis of the low-temperature SC phase with  $T_c^* \simeq 5.6$  K  $\sim T_N$ , coexisting with the commensurate AF structure, suggests a sizable value of the EPI constant  $\lambda_s \sim 0.93$ . We also provide strong support for the recently proposed by us ‘‘Fermi surface (FS) separation’’ scenario for the coexistence of magnetism and superconductivity in magnetic borocarbides, namely, that the superconductivity in the commensurate AF phase survives at a special (nearly isotropic) FS sheet without an admixture of Ho 5d states. Above  $T_c^*$  the SC features in the PC characteristics are strongly suppressed pointing to a specific weakened SC state between  $T_c^*$  and  $T_c$ .

PACS numbers: 72.10.Di, 74.45.+c, 74.70Dd

## INTRODUCTION

Borocarbide superconductors  $RT_2\text{B}_2\text{C}$ , where  $R$  is a rare-earth element and  $T$  is a transition metal element, mainly Ni, (see, e.g., Refs. 1, 2 and further Refs. therein) have been studied intensively during the last decade. However, in spite of their much more simple, less correlated, 3D electronic structure compared with high- $T_c$  materials, the superconductivity in borocarbides is still under debate. Based on the interpretation of many magnetic, muon spin resonance, spectroscopic, specific heat, etc. measurements [1] it is widely accepted that the superconducting (SC) state has an  $s$ -wave symmetry and the pairing is mediated by the electron-phonon (el-ph) interaction. On the other hand for the magnetically ordered borocarbide superconductors the role of the crystal-electric-field (CEF) splitting of the  $4f$ -shell states of the  $R^{+3}$  ion and their excitations are of fundamental importance to understand both ordering phenomena. Additionally, the el-ph interaction responsible for the SC state in these compounds has also been analyzed within the multiband Eliashberg theory [3, 4] with emphasis on the complex Fermi surface with different contribution to the SC state by different orbitals on different Fermi surface sheets [4, 5, 6, 7, 8].

In the family of borocarbide superconductors

$\text{HoNi}_2\text{B}_2\text{C}$  is distinguished: it exhibits a remarkable reentrant superconductivity and a variety of magnetic orderings [1]. The reentrant behavior occurs in a temperature range just above the commensurate antiferromagnetic order at about  $T_N \simeq 5.2$  K and below the temperature  $T_M \simeq 6$  K, which separates the low-temperature magnetic commensurate phase from the high-temperature paramagnetic phase by a not completely resolved yet intermediate incommensurate magnetic phase. In the same temperature range between  $T_N$  and  $T_M$  incommensurate structures do occur: an  $a$ -axis-modulated one and a spiral structure along the  $c$ -axis.

By point-contact (PC) spectroscopic investigations [9] both the SC order parameter and the PC electron-boson(phonon) interaction (EB(P)I) spectral function  $\alpha_{\text{PC}}^2 F(\omega)$  can be determined in studying the first and second derivatives of the  $I(V)$  characteristic of PC’s. The measurement of the second derivative of the  $I(V)$  of PC’s provides straightforward information on the PC EB(P)I function  $\alpha^2 F(\omega)$  [9]. The knowledge of  $\alpha^2 F(\omega)$  for conducting systems is a touchstone to the phonon-mediated superconductivity which is governed mainly by the value of the el-ph-coupling parameter  $\lambda = 2 \int \alpha^2 F(\omega) \omega^{-1} d\omega$ . Moreover, the comparison of the experimentally determined  $\alpha_{\text{PC}}^2 F(\omega)$  with the results of model calculations

could be used to distinguish between different scenarios. Thus the PC spectroscopy could be helpful to illuminate many details of the EPI in  $\text{HoNi}_2\text{B}_2\text{C}$  as well as to resolve other possible quasiparticle interactions, e. g., mediated by magnons and CEF excitations. In addition to this the SC gap determines the behavior of the  $I(V)$  curve for the PC in the energy range of a few meV. Hence, this region is widely used to determine the SC gap from a routine fitting by the well-known Blonder-Tinkham-Klapwijk (BTK) equations [10]. All this potential information should be used to deepen the present sparse knowledge of the SC properties and to help to elucidate the mechanism(s) of superconductivity of the title material.

Up to now,  $\text{HoNi}_2\text{B}_2\text{C}$  has been investigated by PC spectroscopy in [11, 12, 13, 14]. The first three papers are devoted to investigations of the SC gap. In general, standard isotropic BCS (Eliashberg)-type behavior of the gap was found below  $T_N$ , while between  $T_N$  and  $T_c \simeq 8.5\text{K}$  the SC features in PC spectra are strongly suppressed and speculation about some different SC state [11] or ‘gapless’ superconductivity [12] were undertaken. The PC EBI spectra for  $\text{HoNi}_2\text{B}_2\text{C}$  were studied and analyzed in Ref.[14]. There, the main attention was devoted to the study of the low energy part of the spectra and to the investigation and understanding of the so called ‘soft’ mode at about 4 meV in the electron-quasiparticle spectrum. However, the measured spectra were featureless above 20 meV, although a number of pronounced phonon peaks are well resolved at higher energies by neutron spectroscopy [15]. In this study we present more detailed PC EBI spectra of  $\text{HoNi}_2\text{B}_2\text{C}$  in comparison with those mentioned in the Refs. given above including also our recent data presented at two international conferences SCES’04 and M2S-HTSC-VIII [17, 18]. Additionally, to explain our findings with respect to the SC gap we provide support for the separation of magnetism and superconductivity on different Fermi surface sheets in magnetic borocarbides [5, 6, 8].

## EXPERIMENTAL DETAILS

We have used single crystals of  $\text{HoNi}_2\text{B}_2\text{C}$  grown by a floating zone technique with optical heating [19]. The residual resistivity is  $\rho_0 \simeq 3\mu\Omega\text{cm}$  and the residual resistivity ratio  $\text{RRR}=13$ . Final series of measurements were done for sample with improved quality with  $\text{RRR}=19$ . The sample becomes superconducting at about 8.5 K. PCs were established both along the  $c$  axis and in perpendicular direction by standard ‘needle-anvil’ or ‘shear’ methods [9]. As a counter electrode Cu or Ag thin wires ( $\varnothing=0.15\text{mm}$ ) were used. The spectra with resolved phonon features like in Fig.1 were registered by touching of the sharpened Cu wire on a shallow bright caving of about  $1\times 1\text{mm}^2$  on the  $\text{HoNi}_2\text{B}_2\text{C}$  crystal surface (see

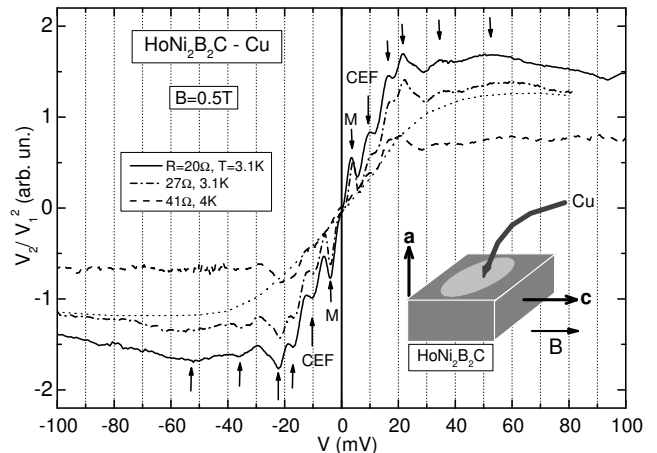


Figure 1: Experimental PC spectra [see Eq. (2)] of several  $\text{HoNi}_2\text{B}_2\text{C}$ -Cu PCs. The dotted curve shows an example of the tentative behavior of the background for the dash-dot curve spectrum. A magnetic field of 0.5 T is applied to suppress superconductivity. The arrows mark a ‘magnetic’ (M) peak at about  $\pm 3\text{mV}$ , a CEF peak, and positions of other resolved peculiarities on the curves maxima. The inset shows a sketch of the PC configuration (see also the text for more details).

inset in Fig. 1). The electron probe microanalysis (WDX mode) has shown that the cavity surface has single phase microstructure and stoichiometric composition well corresponding to the 1:2:2:1 ratio, while excess of Ni has been observed in other places on that crystal surface.

## RESULTS AND DISCUSSION

According to the theory of PC spectroscopy [20] the second derivative  $R^{-1}dR/dV = R^{-2}d^2V/dI^2(V)$  of the  $I - V$  curve of the ballistic contact at low temperatures, where  $R = dV/dI$ , is determined by the PC EPI function  $\alpha_{\text{PC}}^2 F(\omega)$ ,

$$R^{-1} \frac{dR}{dV} = \frac{8ed}{3\hbar v_{\text{F}}} \alpha_{\text{PC}}^2(\omega) F(\omega)|_{\hbar\omega=eV}, \quad (1)$$

where  $d$  is the PC diameter,  $e$  is the electron charge and  $\alpha_{\text{PC}}$ , roughly speaking, measures the interaction of an electron with the phonon branches. This interaction is affected by large angle scattering (back-scattering) processes [20] of electrons in the constriction of the PC. Thus  $\alpha_{\text{PC}}^2 F(\omega)$  is a kind of transport EPI functions which select phonons with a large momentum or umklapp scattering. In practice  $\alpha_{\text{PC}}^2(\omega) F(\omega)$  can be extracted from the measured rms signal of the second  $V_2$  ( $V_2 \propto d^2V/dI^2$ ) harmonic of a small alternating voltage  $V_1$  ( $V_1 \propto dV/dI$

is the first harmonic signal) superimposed on the ramped dc voltage  $V$ , so that from (1):

$$\alpha_{\text{PC}}^2(\omega) F(\omega)|_{\hbar\omega=eV} = \frac{3}{2\sqrt{2}} \frac{\hbar v_{\text{F}}}{ed} \frac{V_2}{V_1^2}. \quad (2)$$

In the case of a heterocontact between two metals the PC spectrum represents a sum of the contributions from both metals 1 and 2 weighted by the inverse Fermi velocities [23]:

$$\frac{V_2}{V_1^2} \propto R^{-1} \frac{dR}{dV} \propto v \frac{(\alpha^2 F)_1}{v_{F1}} + (1-v) \frac{(\alpha^2 F)_2}{v_{F2}}, \quad (3)$$

where  $v$  is the relative volume occupied by metal 1 in the PC. Thus, using of the heterocontacts enables also us to estimate the relative strength of the EBI in the investigated material as compared to some standard or well known case.

To study the SC gap we have measured  $dV/dI$  characteristics of N-c-S PCs (here N denotes a normal metal, c is the constriction and S is the superconductor under study). Then utilizing the generally used Blonder-Tinkham-Klapwijk equations [10] fits of the measured curves have been performed. As fit parameters the SC gap  $\Delta$  and the dimensionless barrier parameter  $Z$  have been used. A possible additional smearing of the  $dV/dI$  curves was also taken into account by including the parameter  $\Gamma$ , usually interpreted as a broadening of the quasiparticle DOS in the superconductor due to finite life-time effects.

### PCS of quasiparticle excitations

Our PC spectra of  $\text{HoNi}_2\text{B}_2\text{C}$  demonstrate clear maxima at about 3, 10, 16 and 22 mV, a smeared maximum at 34 mV, and a hump around 50 mV (Fig. 1). The maxima above 15 mV correspond well to the phonon DOS maxima of the nonmagnetic sister compound  $\text{LuNi}_2\text{B}_2\text{C}$  [15] [see Fig. 2(b)] derived from inelastic neutron scattering data. Only the high energy part of the PC spectrum is remarkably smeared. Fig. 2(a) displays the PC EBI function, obtained from the PC spectrum after subtraction of the background. According to the neutron data [15] there is a gap around 40 meV in the phonon DOS, which separates the acoustic and the optic branches. In this energy region a minimum occurs in our PC spectra.

We have also succeeded to receive PC spectra with well resolved high energy maxima around 50 and 100 mV (see Fig. 3). The position of the 50-mV maximum coincides with the maximum in the phonon DOS for  $\text{LuNi}_2\text{B}_2\text{C}$  shown in Fig. 2b, even the shoulder at about 60 mV is resolved in the PC spectra (this feature is more clear at the negative bias). In the phonon DOS for the nonmagnetic sister compound  $\text{YNi}_2\text{B}_2\text{C}$  a maximum at around

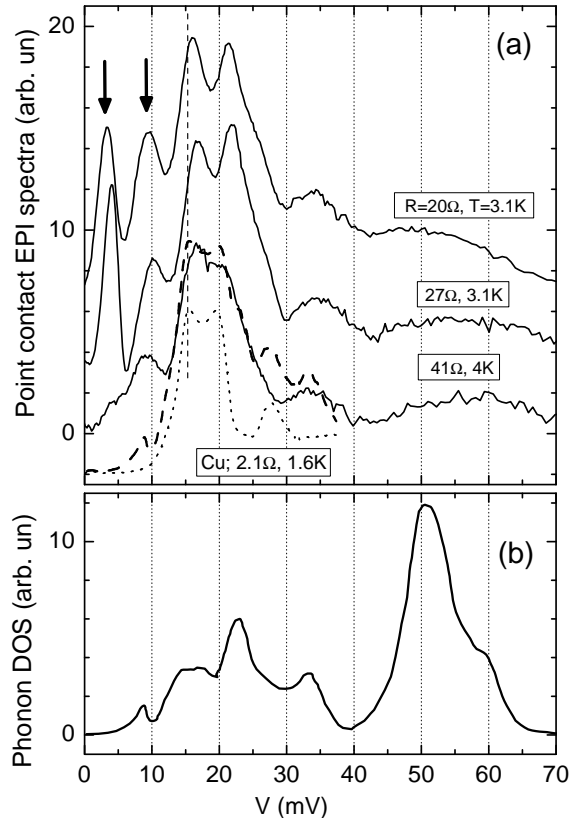


Figure 2: (a) PC spectra from the Fig. 1 with subtracted background (3 upper solid curves). The arrows mark the position of the CEF peak and the ‘magnetic’ peak at about 4 mV, best visible for the two upper curves. The bottom dotted curve shows the PC spectrum of Cu. The vertical dashed line marks the position of the first maximum in the Cu spectrum. The dashed curve presents sum of the PC spectrum of Cu with a function scaled by the phonon DOS from panel (b). (b) The neutron phonon DOS for  $\text{LuNi}_2\text{B}_2\text{C}$  [15].

100 meV has been observed in Ref. 15. It has been attributed to the high-frequency B-C bond stretching vibration in accord with theoretical results obtained in frozen phonon calculations at 106 meV for the zone-center Raman active mode of  $\text{YNi}_2\text{B}_2\text{C}$  [16]. The low-energy part ( $< 30$  meV) of the PC spectra in Fig. 3 shows a less detailed structure as compared to the spectra from Fig. 1. Here maxima only at about 4, 10 and 15 mV are seen. Also a shoulder in the range of 22 meV peak is visible which is more pronounced at negative polarity and as shown for the spectra in the inset. However, in interpreting these spectra we have to take into account for possible contribution of Cu derived phonons since Cu has been used as a counter electrode (needle). The dashed curve in Fig. 2(a) presents the sum of the Cu spectrum and the phonon DOS from Fig. 2(b). It is seen that contributions from Cu may be appreciable for the spec-

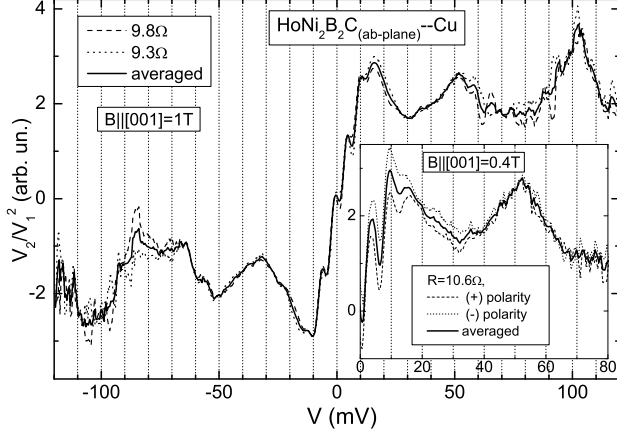


Figure 3: PC spectra of  $\text{HoNi}_2\text{B}_2\text{C}-\text{Cu}$  contact with well resolved high energy maxima around 50 and 100 mV. PC resistance was decreased from  $10.6\Omega$  (spectrum in the insert) to  $9.3\Omega$  (main panel) between successive measurements. In the main panel also averaged for two contacts spectrum (solid line) is shown, while in the inset averaged for the positive and negative bias spectrum of the same contact is shown by solid line. Temperature is 3K and magnetic field is applied to suppress superconductivity.

trum of the  $41\Omega$  contact in the range between 15–20 meV, while the two other spectra have pronounced maxima at 16 and 22 meV, i. e. at energies higher than the maxima in the Cu spectrum at 15 and 20 meV. Moreover, all  $\text{HoNi}_2\text{B}_2\text{C}-\text{Cu}$  spectra contain no visible contribution from the weaker Cu peak at about 27 meV, therefore we conclude that a contribution of Cu is unsubstantial at least for the two upper spectra in Fig. 2(a). Apparently, the low Fermi velocity in nickel borocarbides [1] as compared to the noble metals accentuate the intensity of  $\text{HoNi}_2\text{B}_2\text{C}$  features according to Eq. (3). Contrary, the PC spectra in Fig. 3 have likely a contribution from Cu derived phonons in the region 15–20 mV, which masks the expected  $\text{HoNi}_2\text{B}_2\text{C}$  phonon maxima so that the 22 meV maximum looks like a broad shoulder. In Fig. 3(inset) also the asymmetry of the spectra versus bias voltage polarity is clearly seen in the energy region of Cu phonons, which is characteristic for heterocontact, if the contribution from both electrodes to the spectrum is comparable [9].

The most prevalent type of  $\text{HoNi}_2\text{B}_2\text{C}$  PC spectrum is shown in Fig. 4. Here a maximum close to 3 mV and another one around 10 meV are dominant. The latter maximum might be connected with CEF excitations, observed in this range by inelastic neutron scattering studies [24, 25, 26]. The maximum around 3 meV is associated with a magnetically ordered state, since it disappears above the Néel temperature mainly in the range

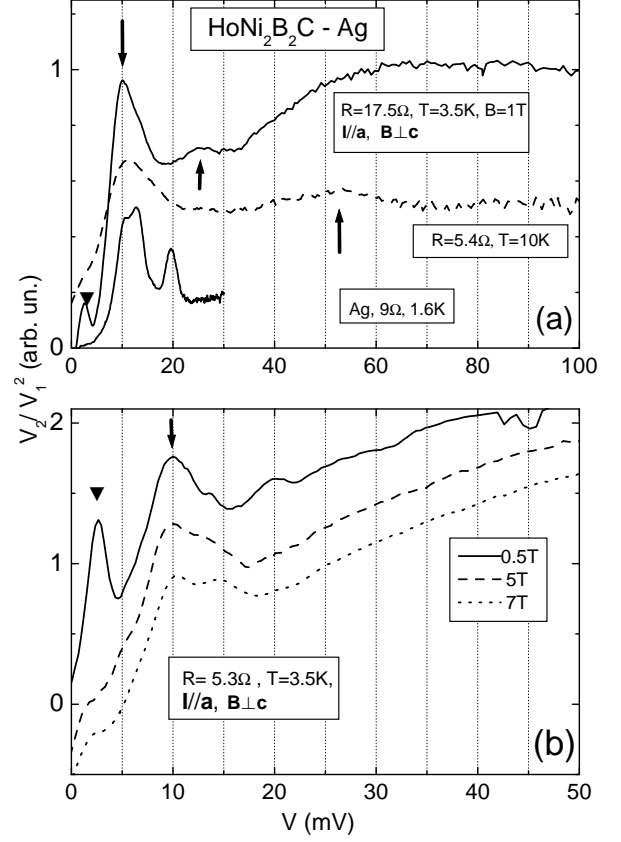


Figure 4: PC spectra [see Eq. (2)] of several  $\text{HoNi}_2\text{B}_2\text{C}-\text{Ag}$  PCs with a dominant 10-mV peak (the  $\downarrow$  marks the CEF peak, the  $\uparrow$  mark the position of the main phonon peaks from Fig. 2b, the black triangle marks the ‘magnetic’ peak at about 4 meV): (a) two spectra with a dominant 10-meV peak. In the first case the superconductivity is suppressed by magnetic fields, in the second case – by high temperature. The latter curve is measured on a cleaved small piece of a  $\text{HoNi}_2\text{B}_2\text{C}$  single crystal. The bottom curve shows the PC spectrum of Ag. (b) The modification of the spectrum with a dominant 10-mV peak for various applied magnetic fields.

8–10 K (see dashed curve in Fig. 4(a)) and it can be suppressed by a magnetic field of a few Tesla (see Fig. 4(b)). A detailed discussion of the origin of this peak will be given in the next section. At the energy of about 10 meV a contribution from the first peak in the phonon DOS could also be expected. For  $\text{LuNi}_2\text{B}_2\text{C}$  the first phonon peak is observed at about 9 meV (see Fig. 2(b)). For the lighter (about 6%) Ho ions the peak position may be somewhat shifted to higher energies. Note also that the measured phonon dispersion curves  $\omega(q)$  for  $\text{HoNi}_2\text{B}_2\text{C}$  [27] have a tendency that  $\partial\omega(q)/\partial q \rightarrow 0$  around 10–12 meV pointing to an enhanced phonon DOS (or maximum) in this region. However, we have observed that the 10-mV maximum is considerably affected by a magnetic field (see Fig. 4(b)), therefore a contribution of CEF ex-

citations to the 10-meV peak seems to be appreciable. Unfortunately, due to ‘magnetic forces’ it was difficult to keep the mechanical contact stable in magnetic fields above 5 T, especially when the field direction was out of the  $c$ -axis. Therefore the influence of the magnetic field on the 10-meV peak (to separate CEF and phonon contribution to this peak) could be investigated only qualitatively so far.

The spectra discussed here demonstrate weak and smeared phonon maxima above 10 mV (see arrows in Fig. 4(a)) in contrast to the spectra shown in Fig. 2(a), but they have a pronounced 10-mV peak (see Fig. 4), which points to the importance of CEF excitations in the transport properties of HoNi<sub>2</sub>B<sub>2</sub>C. Besides, the electron-CEF interaction may be also important for a complete understanding of the mechanism of superconductivity in this compound. We emphasize that the spectra with the dominant 10-mV peak were qualitatively the same independent of the counter electrode (Ag or Cu) which discards remarkable contribution to the PC spectra from these metals (see the PC spectra of Cu and Ag in Figs. 2a and 4a).

From the measured EBI function (see Fig. 2(a)) the EBI parameter  $\lambda_{\text{PC}} = 2 \int \alpha_{\text{PC}}^2 F(\omega) \omega^{-1} d\omega$  was calculated, which was found to be smaller than 0.1 only. However, there are large uncertainties in the determination of  $\lambda_{\text{PC}}$  if heterocontacts are used. First, this is because the relative volume  $v$  occupied by the investigated sample in a PC can deviate from 1/2 [see (3)]. Secondly, the deviation from the ballistic regime in PCs has to be corrected by a pre-factor  $l_i/d$  in (3), where  $l_i$  is the elastic electron mean free path and  $d$  is the PC diameter. However,  $l_i$  is difficult to evaluate for PC. Further, the available PC theory and all its equations such as Eq. (2) have been derived in the framework of the free electron model and a single-band Fermi surface. Then, paying attention that the contribution of Cu in the PC spectra of HoNi<sub>2</sub>B<sub>2</sub>C-Cu heterocontacts in Fig. 2(a) is hardly to be resolved we can conclude that the intensity of the EBI function in HoNi<sub>2</sub>B<sub>2</sub>C has to be larger than that in Cu, where  $\lambda_{\text{PC}} \simeq 0.25$  [9]. This provides a complementary confirmation of the moderate strength of the EBI in HoNi<sub>2</sub>B<sub>2</sub>C with a lower bound of 0.25 for  $\lambda_{\text{PC}}$  [30]. Moreover the 10-mV peak contributes about 20-30% to the  $\lambda$  value indicating that CEF excitations should be taken into account to understand the SC properties of HoNi<sub>2</sub>B<sub>2</sub>C. The contribution of the high frequency modes to  $\lambda$  can be estimated from the spectra in Fig. 3. It amounts about 10% for each of the 50 and 100 mV maxima. Note, that by estimating  $\lambda$  we discard the contribution of the ‘magnetic’ peak around 3 mV, the nature of which is under discussion (see below).

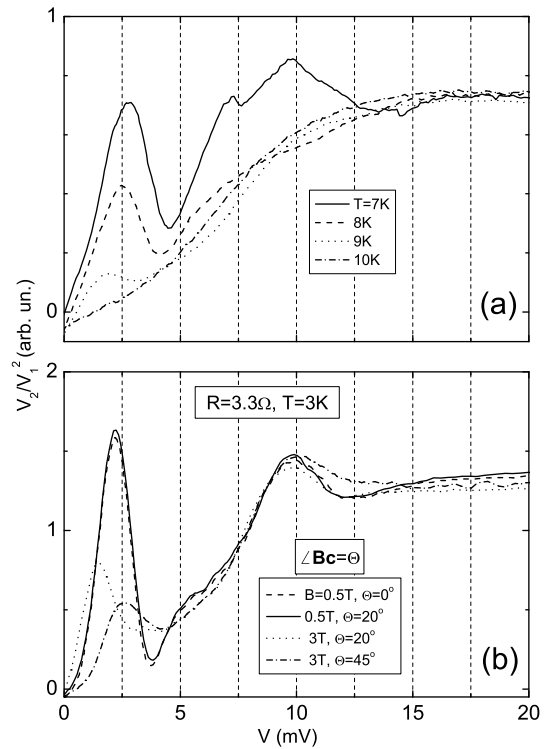


Figure 5: (a) PC spectra [see Eq. (2)] of HoNi<sub>2</sub>B<sub>2</sub>C-Cu contact established along the a-axis at different temperature. (b) PC spectra of HoNi<sub>2</sub>B<sub>2</sub>C-Ag contact established along the a-axis with varying of the magnetic field direction relative to the  $c$ -axis.

### ‘Magnetic’ peak

Let us turn to the low energy maximum around  $eV_M \approx 3$  meV. As we mentioned above it is very probably related to a magnetic ordering, since it disappears at temperatures  $T_M \sim 8-10$  K (see Fig. 5(a)) and it can be suppressed by an external magnetic field (Fig. 5(b)). Figure 5(b) shows that by increasing the angle between the applied magnetic field and the  $c$ -axis, the height of the maximum goes down and its position changes. Thus, this maximum is more robust, if the field is applied along the  $c$ -axis. This is in line with the result reported in Ref. 28 that for a field along the  $c$ -axis the antiferromagnetic phase with  $T_N \simeq 5$  K is robust up to quite large fields, while for the perpendicular directions this antiferromagnetic phase is already suppressed above  $B=0.5$  T at  $T=3$  K. For our PCs both  $T_M$  and the magnetic field which suppresses the ‘magnetic’ peak are higher. In particular, especially the magnetic field is enhanced which reaches here up to 5 T (see Fig. 4(b)). In this context it should be mentioned that inside a PC a remarkable (uniaxial) pressure can be created. This might cause an

increase of  $T_N$  with a ratio up to  $dT_N/dP \simeq 8 \text{ K/GPa}$  [29].

For completeness it should be mentioned that spectra with a dominant 3 meV peak (its position may vary between 2.5 and 5 meV) and the practically absence of any other maxima were observed on uncleaved ‘as-grown’ surfaces of  $\text{HoNi}_2\text{B}_2\text{C}$ . Later on the electron probe microanalysis showed deviations from the stoichiometry on this surface, which can modify both  $T_N$  and the characteristic magnetic field. As mentioned in Ref. 19 crystallographically oriented thin plates of the nonsuperconducting  $\text{HoNiBC}$  compound have been observed in selected parts of as-grown  $\text{HoNi}_2\text{B}_2\text{C}$  crystals. It is well-known that the 1:1:1:1 compound  $\text{HoNiBC}$  exhibits long-range magnetic order below  $T_N \simeq 10 \text{ K}$  [31]. Therefore, the observation of a ‘magnetic’ peak persisting up to 10 K may be connected with admixture of 1:1:1:1 phase.

Thus, the origin of the ‘magnetic’ peak in the PC spectra has to be still under debate and we will consider further scenarios. It could be connected with a transition to the thermal regime by a voltage rise, which produces peak-like features in the PC spectra at  $eV_M \simeq 3.63k_B T_M$  (here  $T_M$  is a magnetic transition temperature) as it was shown for ferromagnetic metals [32]. However, this is not likely the case, because an increase of temperature in the PC would drastically smear the phonon maxima in the spectra as well. On the other hand, it was shown in Ref. 33 that the reabsorption of nonequilibrium phonons generated by electrons in a PC leads to a lattice heating up to a temperature of  $eV/4$  (and the appearance of a background in the PC spectra), however, here the electron gas of the conduction electrons should remain cold preventing a smearing of the PC spectra whereas the local  $\text{Ho } 4f$  moments might be affected due to a strong enough magnetoelastic coupling [21, 22]. We suppose that such a ‘heating’ by nonequilibrium phonons suppresses the magnetic order. The destruction of the antiferromagnetic order in  $\text{HoNi}_2\text{B}_2\text{C}$  leads to a sharp increase of the resistivity at  $T_N$  (see, e. g., Fig. 3 in Ref. 28), which manifests itself in the PC spectra as a peak-like feature. Indeed, the position of the peak around  $2.5 \text{ meV}$  (see Fig. 5) corresponds to the temperature  $eV_M/4 \simeq 7 \text{ K} \sim T_N$ .

### PCS of the SC energy gap in the commensurate antiferromagnetic phase

For the N-c-S metallic junctions (here N denotes a normal metal, c is the constriction and S is a superconductor) under consideration also the SC energy gap  $\Delta$  can be investigated (see, e.g., [9], Chapter 3.7). The SC gap manifests itself in the  $dV/dI$  characteristic of a N-c-S contact as pronounced minima around  $V \simeq \pm\Delta$  at a temperature well below  $T_c$ . Such  $dV/dI$  curves are presented in Fig. 6. Using the BTK equations [10] to fit  $dV/dI$ , the SC gap  $\Delta$  and its temperature dependence are established (see Fig. 6). It is seen that  $\Delta(T)$  has a BCS-type depen-

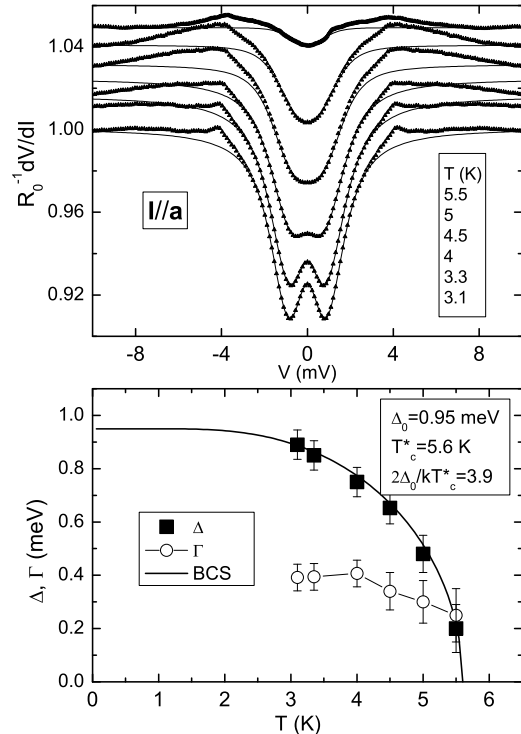


Figure 6: Upper panel:  $dV/dI$  curves (symbols) of  $\text{HoNi}_2\text{B}_2\text{C}$ -Cu contact ( $R = 2.7 \Omega$ ) established along a-axis with varying temperature. PC spectra for this contact are shown in Fig. 5(a). Solid lines are BTK fitting curves. Bottom panel: temperature dependence of the SC energy gap  $\Delta$  and ‘smearing’ parameter  $\Gamma$  at  $B=0 \text{ T}$  obtained by a BTK-like fitting of the curves shown in the upper panel at constant ‘tunneling’ parameter  $Z \approx 0.5$ . Solid smooth line is the BCS curve.

dence, however the temperature where the gap vanishes  $T_c^* \simeq 5.6 \text{ K}$  is well below  $T_c \simeq 8.5 \text{ K}$  of the bulk crystal, i.e., the gap disappears close to  $T_N$ . Similar observation of a gap which vanishes at few Kelvin below  $T_c$  were presented in [11, 12] both for poly- and single crystals of  $\text{HoNi}_2\text{B}_2\text{C}$ . In Ref. [12] the authors supposed a gapless state between  $T_c^*$  and  $T_c$  based on the observation of an abrupt suppression of SC features in  $dV/dI$  when crossing  $T_c^*$  and the failure of a BTK fit above  $T_c^*$  [34]. Note, that in the mentioned temperature range  $\text{HoNi}_2\text{B}_2\text{C}$  exhibits [1] a specific magnetic spiral structure. According to [35, 36] the helical magnetic order weakens the superconductivity and even nonmagnetic impurities do suppress superconductivity in systems with coexisting superconductivity and antiferromagnetism [37].

We would like also to accentuate that the same gap value with a similar temperature and magnetic field behavior has been found for a cleaved surface of the same

HoNi<sub>2</sub>B<sub>2</sub>C single crystal with an Ag counter electrode, that is for some arbitrary direction. This observation together with analogous data for  $\Delta$  from [11, 12] both for poly- and single HoNi<sub>2</sub>B<sub>2</sub>C crystals demonstrates at least a small gap anisotropy and a reasonable physical meaning of  $T_c^*$ . Therefore we adopt the "Fermi surface separation" scenario for the coexistence of magnetism and superconductivity in magnetic borocarbides, i.e. their coexistence on different Fermi surface sheets (FSS), proposed in Refs. [5, 6, 8]. In other words, we suggest that the superconductivity in the commensurate antiferromagnetic phase survives only at a special (nearly isotropic) FSS with no admixture of Ho  $5d$  states. The latter mediate the magnetic exchange interaction between the localized Ho  $4f$  moments and a part of the delocalized conduction electrons for which a standard  $s$ -wave superconductivity is easily to be destroyed or strongly suppressed. Such a magnetic link between the Ho  $4f$  moments provided by conduction electrons is necessary for the RKKY interactions to explain the observed magnetic orderings at relative high temperatures. In order to proceed with a semi-quantitative analysis of our PC data, we may now adopt the well understood standard isotropic single band (ISB) model to analyse the residual superconductivity. From the measured gap value  $\Delta_0=0.95$  meV and the estimated  $T_c^* \approx 5.6$  K (or the slightly different value of 5.8 K as discussed below) remarkable strong coupling corrections can be estimated. Starting for instance from a relation first derived by Geilikman and Kresin [38, 39]

$$\frac{2\Delta(0)}{k_B T_c} = 3.53 \left[ 1 + 12.5 \left( \frac{k_B T_c}{\hbar\omega_l} \right)^2 \ln \left( \frac{\hbar\omega_l}{2k_B T_c} \right) \right], \quad (4)$$

one estimates a relatively low value for the logarithmically weighted phonon frequency  $\hbar\omega_l \approx 10$  meV. Using the well-known Allen-Dynes expression for the critical temperature we may estimate the effective electron-boson coupling constant  $\lambda_s$  as 0.934 adopting a typical value for the Coulomb pseudopotential  $\mu^*=0.13$ . Then, from the estimated upper critical field  $H_{c2}(0) \approx 0.8$  T one estimates in the clean limit the effective Fermi velocity  $v_F$  according to [40]

$$v_F [10^5 \text{m/s}] = 0.154 \frac{T_c [\text{K}] (1 + \lambda)^{1.1}}{\sqrt{H_{c2}(0) [\text{T}]}}, \quad (5)$$

as a lower bound  $v_F \approx 2.06 \times 10^5$  m/s. A similar value  $v_F \approx 1.91 \times 10^5$  m/s follows, if  $H_{c2}(0) \simeq 0.93$  T is estimated from the slope of  $dH_{c2}/dT$  near  $T_c$  using the well-known WHH-relation between the former two quantities. These estimates may be helpful to elucidate which of the FSS does bear the residual superconductivity. Compared with the nonmagnetic borocarbides ( $\lambda \sim 1.2$  to 1.4) the obtained coupling constant is surprisingly less suppressed and the low value  $\hbar\omega_l \approx 10$  meV indicates that most of the phonon modes above 10 meV shown in Fig. 2 should

be regarded as relevant for those nonactive FSS's where the superconductivity has been extruded by the rare earth induced magnetism. Since in the scenario under consideration the pairing comes mainly from the interaction with low-frequency bosonic modes, the observed peak near 10 meV and its decomposition into contributions from different bosons deserves special interest. In particular, assuming that the remaining superconducting FSS couples dominantly to the modes which contribute to the 10 meV peak, a non-negligible contribution  $\lambda_{s,\text{CEF}}$  from the attractive interaction with crystal-field excitations (i.e. from the inelastic asymmetric Coulomb scattering as proposed by Fulde [41]) would be rather challenging. Regarding the exact frequency values of the relevant bosonic modes, the large sensitivity of Eq. (4) to the actual  $T_c$  value should be stressed. In this context the rather similar values of  $T_c \approx 6.1$  K,  $H_{c2}(0) \approx 0.75$  to 0.9 T [42, 43] and  $2\Delta(0)/k_B T_c \approx 3.81$  for DyNi<sub>2</sub>B<sub>2</sub>C are noteworthy (see Ref. 43 Fig.6). Here  $\hbar\omega_l \approx 9.9$  meV and  $\lambda_s = 0.939$  (for  $\mu^* = 0.13$ ) can be derived from Eq. (4) and the Allen-Dynes  $T_c$ -formula.

Such a similarity between HoNi<sub>2</sub>B<sub>2</sub>C and DyNi<sub>2</sub>B<sub>2</sub>C seems to be natural because the same commensurate antiferromagnetic phase is probed for both closely related systems which exhibit within the LDA (local density approximation) nearly the same electronic structure [44]. Also similar phonon spectra are expected. In this context, in comparing the two SC phases which coexist with the same commensurate antiferromagnetic phase in HoNi<sub>2</sub>B<sub>2</sub>C and DyNi<sub>2</sub>B<sub>2</sub>C, the violation of the frequently used De Gennes-scaling for magnetic borocarbides [1] is striking. This scaling employs the scaling factor DG defined as

$$DG = (g_L - 1)^2 J(J + 1), \quad (6)$$

where  $g_L$  is the Landé-factor and  $J$  denotes the magnetic moment at the rare earth site. According to that standard scenario an *enhanced* SC state would be expected for the low-temperature SC phase of HoNi<sub>2</sub>B<sub>2</sub>C. However, by comparing the SC transition temperatures and gap values of the magnetically adjacent borocarbides contradictory results are derived. The PC-data for ErNi<sub>2</sub>B<sub>2</sub>C [45] yield  $\Delta(0)_{Er} \approx 1.7$  meV (ignoring a weak anisotropy of  $H_{c2}$ ), the gap of DyNi<sub>2</sub>B<sub>2</sub>C amounts to  $\Delta(0)_{Dy} \approx 1.0$  meV and  $\Delta(0)_{Er} > \Delta(0)_{Ho} > \Delta(0)_{Dy}$  with  $T_{c,Er} = 10$  K  $>$   $T_{c,Ho} = 8.5$  K  $>$   $T_{c,Dy} = 6$  K is expected. This is in contrast with the measured value of 0.95 meV for HoNi<sub>2</sub>B<sub>2</sub>C. Anyhow, the measured relation  $\Delta(0)_{Ho} \leq \Delta(0)_{Dy}$  suggests that the residual superconductivity below 6 K is not affected by the usual magnetic pair breaking. Our FSS-related coexistence picture allows also a new interpretation of the specific heat data reported by Michor *et al.* [46]: using the estimates for DyNi<sub>2</sub>B<sub>2</sub>C given above, strong coupling corrections for

the relative specific heat jump [39]

$$\frac{\Delta C}{\gamma_s k_B T_c} = 1.43 \left[ 1 + 53 \left( \frac{k_B T_c}{\hbar \omega_l} \right)^2 \ln \left( \frac{\hbar \omega_l}{3 k_B T_c} \right) \right], \quad (7)$$

can be used to estimate the partial density of states  $\gamma_s \propto N_s(0)(1 + \lambda_s)$  of the electronic subgroup involved in the SC transition. The observed reduced SC specific heat jump of  $\Delta C \approx 70$  mJ/molK for DyNi<sub>2</sub>B<sub>2</sub>C, that corresponds to a partial density of states of about  $N_s(0) = 4.16$  mJ/molK<sup>2</sup>, only, to be compared with about  $N_{tot}(0) = 10$  mJ/molK<sup>2</sup> for the total density of states as derived from LDA band structure calculations for nonmagnetic and magnetic borocarbides [44].

It is interesting to compare  $\lambda_{PC}$  with the superconducting coupling constant  $\lambda_s$  derived above as well as with superconducting and high-temperature resistivity data which yield  $\lambda_{tr}$  for related systems in order to understand to which extent  $\lambda_{PC}$  probes the el-ph coupling for all bands. Recent PC measurements for DyNi<sub>2</sub>B<sub>2</sub>C [47] and YNi<sub>2</sub>B<sub>2</sub>C [48] in the best junctions yield a significant larger (smaller) experimental coupling constant  $\lambda_{PC} = 0.4$  (0.1), respectively, compared to the present case with  $\lambda_{PC} = 0.25$  for HoNi<sub>2</sub>B<sub>2</sub>C. However, very often the coupling constants derived from point-contact spectra should be considered as lower bounds for the coupling constants relevant for superconductivity, say  $\lambda_{PC} \approx (0.5$  to  $0.7)\lambda_s$ , which can be derived from different Eliashberg functions  $\alpha^2(\omega)F(\omega)$  extracted by the inversion of usual superconductor tunneling data or from an analysis of the Sommerfeld constant of the linear specific heat in the normal state. Since a value of  $\lambda_s \sim 1.2$  for the case of the non-magnetic borocarbides and  $\lambda_{tr} \approx 0.8$ - $0.9$  for magnetic borocarbides [28] seems to be realistic, we adopt for ideal ballistic contacts  $\lambda_{PC} \sim \lambda_{tr} \approx 0.7$  to  $0.8$  for all Ni-1221 borocarbides under consideration. In fact, the coupling constants, measured by point-contact spectroscopy in the normal state can be regarded as effective single-band properties, i.e. for the multiband system under consideration generalizing Eq. (1), each band (FSS) produces a weighting factor given by the ratio of the corresponding conductances and the Fermi velocities  $v_i$  which in a free electron-like picture reads

$$\lambda_{PC} = \frac{v_{eff}}{\sigma_{tot}} \sum_i \left[ \frac{\sigma_i}{v_i} \lambda_{PC,i} \right], \quad (8)$$

where the band index ' $i=1,..$ ' has been introduced. In the present case following our coexistence scenario we divide the borocarbides under consideration into a magnetic ( $i=1$ ) and a superconducting subsystem ( $i=2$ ) with  $v_{eff} \approx 1.8v_2$  used in calibrating the point-contact spectra and adopt  $v_1 \sim 3v_2$ , as suggested by the LDA-FPLO calculations, one estimates  $\sigma_i/\sigma_{tot} = 0.9$  and  $0.1$ , respectively. Then Eq. (8) can be rewritten as  $\lambda_{PC} = 0.18(3\lambda_1 + \lambda_2)$ . For  $\lambda_1 \sim \lambda_2$  a moderate contribution of

about 25% for the superconducting subsystem to the total  $\lambda_{PC}$  follows. The latter is dominated by the quenched magnetic subsystem for HoNi<sub>2</sub>B<sub>2</sub>C and other magnetic borocarbides. Anyhow, the 10 meV peak can be attributed completely to the residual superconducting subsystem. A similar result was obtained for a specific heat analysis of HoNi<sub>2</sub>B<sub>2</sub>C [49], where the peak near 10 meV was estimated to contribute about 25% to the total coupling constant of 1.2. Related problems and more detailed further comparisons with DyNi<sub>2</sub>B<sub>2</sub>C, ErNi<sub>2</sub>B<sub>2</sub>C, and other magnetic borocarbides will be considered elsewhere.

For completeness and for comparison with Eq. (8) we show the corresponding multiband expressions for the renormalization of the electronic specific heat (the Sommerfeld constant  $\gamma$ ) and the resistivity

$$\lambda_\gamma = \sum_i \frac{N_i(0)}{N_{tot}(0)} \lambda_{\gamma_i}, \quad (9)$$

where  $N_i(0)$  denotes the partial electronic density of states at the Fermi level. Finally, ignoring interband scattering for the high-temperature resistivity where  $\rho(T) \propto \lambda_{tr}T$  one obtains from a straightforward generalization of the well-known Ziman-formula

$$\lambda_{tr} = \left( \sum_i \frac{\omega_{pl,i}^2}{\Omega_{pl,tot}^2} \frac{1}{\lambda_{tr,i}} \right)^{-1}, \quad (10)$$

where  $\omega_{pl}$  denotes the plasma frequency. Thus, in all discussed cases the effective one-band coupling constants are differently decomposed into the partial coupling constants depending on which quantity is probed experimentally.

Lets turn to the magnetic field measurements shown in Fig.7. In contrast to the PC data reported in Ref. 12, where  $\Delta$  initially increases ( $\sim 10\%$ ) in magnetic fields before it drops off to zero, in our case  $\Delta(B)$  exhibits a conventional behavior. decreasing with overall negative curvature (see Fig. 7). Similarly, the excess current  $I_{exc}$ , which is proportional to the gap maximum area in  $dI/dV$  (see Fig. 8 and the figure caption therein), exhibits a temperature dependence (not shown) like  $\Delta(T)$  from Fig. 6, that is  $I_{exc}(T)$  has also a negative curvature. (We remind the reader, that the excess current of an S-c-N contact is governed by  $\Delta$  [50] or the SC order parameter [51].) Contrary,  $I_{exc}(B)$  decreases nearly linearly with the magnetic field (Fig. 8). This is in contrast with the observed pronounced positive curvature of  $I_{exc}(B)$  in MgB<sub>2</sub> [52] and YNi<sub>2</sub>B<sub>2</sub>C [53], where at least two bands are superconducting. Thereby, the observed behavior of  $I_{exc}(B)$  is in line with our scenario that superconductivity survives on separate (one or similar) FSS. In addition to the "vortex" model proposed in [52], the  $I_{exc}(B)$  dependence might be also related to a complex vortex structure for a system with normal and superconducting FSS's as we



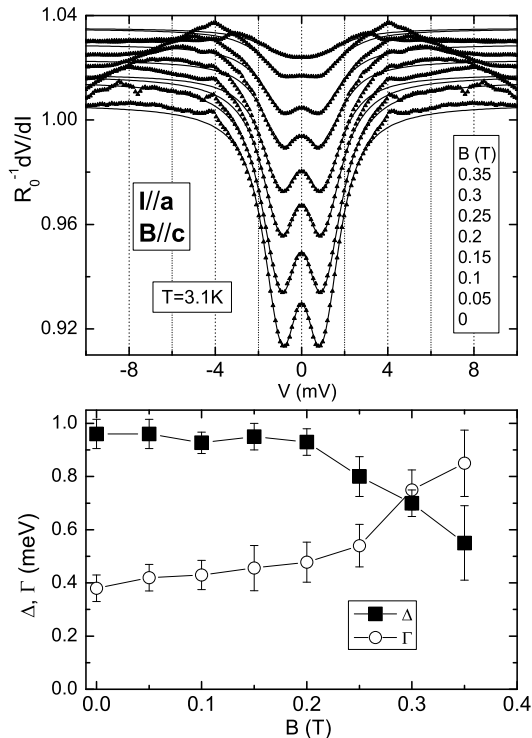


Figure 7: Upper panel: The  $dV/dI$  curves (symbols) for the same  $\text{HoNi}_2\text{B}_2\text{C}$ -Cu contact as employed in Fig. 6 but exposed to an external magnetic field. The solid lines are BTK fitting curves. Bottom panel: the magnetic field dependencies of the SC energy gap and  $\Gamma$  at constant  $Z \approx 0.5$  obtained by BTK-like fits of the curves shown in the upper panel.

suppose in our case. To the best of our knowledge this vortex problem has not been studied so far theoretically.

## CONCLUSION

We have carried out investigations of the EBI spectral function and the SC energy gap in  $\text{HoNi}_2\text{B}_2\text{C}$  by PC spectroscopy. We succeeded to measure PC EBI spectra of  $\text{HoNi}_2\text{B}_2\text{C}$  with distinct phonon features above 15 mV along with additional low energy maxima of non-phonon nature below 15 meV. For the first time the high energy maxima at about 50 meV and 100 meV are clearly observed. Hence, the high energy phonons can not be disregarded by analyzing thermodynamic, electron transport and SC phenomena in the nickel borocarbides. The phonon maxima in the PC spectra correspond well to those in the phonon DOS spectra of borocarbides measured by inelastic neutron scattering. On the other hand the maximum at about 10 meV contains likely also an essential contribution from CEF excitations, while the

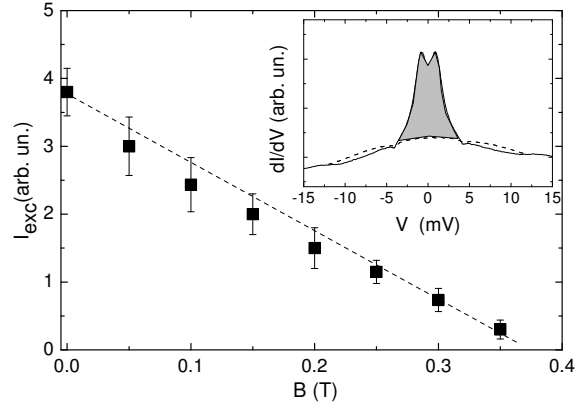


Figure 8: Excess current  $I_{\text{exc}}$  behavior versus magnetic field (symbols) for PC data used also in Fig. 7. Dashed straight line connects two edge symbols. The inset explains the determination of the excess current, which is proportional to the integral intensity of  $dI/dV$  maximum (the shaded area) after subtracting of the normal state  $dI/dV$  (dashed curve) measured at 0.5 T.

low-lying peak around 3 meV is suppressed by temperature and magnetic field rise. Moreover, the peak intensity depends on the angle between the magnetic field and the  $c$ -axis. All these observations point to a ‘magnetic’ origin of this peak, i. e., the peak reflects possibly a transition from the low temperature magnetically ordered state to dis- (or low)- ordered states driven by nonequilibrium phonons generated by accelerated electrons.

The SC gap exhibits in general a ‘conventional’ single-band like standard BCS behavior below  $T_c^* \simeq 5.6$  K with  $2\Delta/k_B T_c^* \simeq 3.9$  pointing to an intermediately strongly coupled SC state. The large similarity of this low-temperature phase with the behavior of  $\text{DyNi}_2\text{B}_2\text{C}$  where superconductivity and a simple commensurate antiferromagnetic state coexist, clearly points to a nonstandard (in the sense of the frequently used De Gennes scaling) suppression of the former compared with nonmagnetic borocarbides. We addressed the specific role of selected Fermi surface sheets and CEF-excitations in this particular case. Between  $T_c^*$  and the upper critical temperature  $T_c \simeq 8.5$  K the SC signal in  $dV/dI$  is drastically suppressed, which explains the difficulties to derive the SC order parameter (or a SC gap) by fitting the  $dV/dI$  data. Hence the SC state between  $T_c^*$  and  $T_c$ , in the region of peculiar magnetic order, is seemingly ‘unconventional’. Due to its weakness there is a large sensitivity to both external effects (stress or pressure by PC creation, high current density in PC) and to the intrinsic properties (small deviation from stoichiometry, a specific SC state at the surface caused by, e.g., peculiar magnetic ordering). Further investigations are desirable to settle

the nature of the SC state in this special temperature range to obtain finally a similar level of understanding as for the low-temperature SC phase coexisting with the commensurate antiferromagnetic state we have achieved here. In a more general context one may only agree with the conclusion drawn in a very recent review paper [2] as to "the  $RNi_2B_2C$  series will continue to provide insight to superconductivity and its interaction and response to local moment magnetism for years, and possibly decades to come."

### Acknowledgements

The support by the Deutsche Forschungsgemeinschaft (SFB 463) and the State Foundation of Fundamental Research of Ukraine are acknowledged. One of the authors (O.E.K.) was supported by the DAAD through a NATO-Grant. We are indebted to L. V. Tyutrina for the help in fitting the  $dV/dI(V)$  data and W. Löser for a critical reading of the manuscript. Discussions with K.-H. Müller, M. Schneider and H. Rosner are acknowledged.

- 
- [1] K.-H. Müller, V. N. Narozhnyi, Rep. Prog. Phys. **64**, 943 (2001); K.-H. Müller, G. Fuchs, S.-L. Drechsler and V. N. Narozhnyi, in: "Magnetic and Superconducting Properties of Rare Earth Borocarbides of the Type  $RNi_2B_2C$ ", Handbook of Magnetic Materials, (Ed. K. H. J. Buschow), Elsevier North-Holland, Vol. 14, (2002), pp. 199-305.
- [2] S.-L. Bud'ko and P.C. Canfield. C.R. Physique **7**, 56 (2006).
- [3] S. V. Shulga, S.-L. Drechsler, G. Fuchs, K.-H. Müller, K. Winzer, M. Heinecke, and K. Krug, Phys. Rev. Lett. **80**, 1730-1733 (1998).
- [4] S.-L. Drechsler, S. V. Shulga, K.-H. Müller, G. Fuchs, J. Freudenberger, G. Behr, H. Eschrig, L. Schultz, M.S. Golden, H. von Lips, J. Fink, V. N. Narozhnyi, H. Rosner, P. Zahn, A. Gladun, D. Lipp, A. Kreyssig, M. Loewenhaupt, K. Koepnik, K. Winzer, K. Krug, Physica C **317-318**, 117 (1999).
- [5] S.-L. Drechsler, H. Rosner, S. V. Shulga, I. Opahle, H. Eschrig, J. Freudenberger, G. Fuchs, K. Nenkov, K.-H. Müller, H. Bitterlich, W. Löser, G. Behr, D. Lipp, and A. Gladun, Physica C **364** 31 (2001).
- [6] S.-L. Drechsler, I. Opahle, S.V. Shulga, H. Eschrig, G. Fuchs, K.-H. Müller, W. Löser, H. Bitterlich, G. Behr, and H. Rosner, Physica B **329**, 1352 (2003).
- [7] S.-L. Drechsler, H. Rosner, I. Opahle, and H. Eschrig, Physica C **408**, 104 (2004).
- [8] A. O. Shorikov, V. I. Anisimov and M. Sgrist, J. Phys.: Condens. Matter **18**, 5973 (2006).
- [9] Yu. G. Naidyuk and I.K. Yanson, *Point-Contact Spectroscopy*, Springer Series in Solid-State Sciences, Vol.145 (Springer Science+Business Media, Inc, 2005).
- [10] G. E. Blonder, M. Tinkham, T. M. Klapwijk, Phys. Rev. B **25**, 4515 (1982).
- [11] L. F. Rybaltchenko, I. K. Yanson, A. G. M. Jansen, P. Mandal, P. Wyder, C. V. Tomy, D. M. Paul, Europhys. Lett. **33**, 483 (1996).
- [12] L. F. Rybaltchenko, A. G. M. Jansen, P. Wyder, L. V. Tyutrina, P. C. Canfield, C. V. Tomy, D. M. Paul, Physica C **319**, 189 (1999).
- [13] A. Andreone, F. Fontana, M. Iavarone, M. Salluzzo, R. Vaglio, J. Low Temp. Phys. **107**, 527 (1997).
- [14] I. K. Yanson, V. V. Fisun, A. G. M. Jansen, P. Wyder, P. C. Canfield, B. K. Cho, C. V. Tomy, D. M. Paul, Low Temp. Phys. **23**, 712 (1997).
- [15] F. Gompf, W. Reichardt, H. Schober, B. Renker, M. Buchgeister, Phys. Rev. B **55**, 9058 (1997).
- [16] H. Rosner, S.-L. Drechsler, K. Koepnik, I. Opahle, and H. Eschrig, in "Rare Earth Transition Metal Borocarbides (Nitrides): Superconducting, Magnetic and Normal State Properties" (Eds. K.-H. Müller and V. Narozhnyi), Kluwer Academic Publishers Dordrecht, NATO Science Series "II. Mathematics, Physics and Chemistry", V. 14 (2001) pp. 71-82.
- [17] Yu. G. Naidyuk, O. E. Kvitnitskaya, I. K. Yanson, G. Fuchs, K. Nenkov, S.-L. Drechsler, G. Behr, D. Souptel, K. Gloos, Physica B **359-361**, 469 (2005).
- [18] A part of the data reported here has been presented within an invited talk at the M<sup>2</sup>S-HTSC Conference in Dresden (July 9-14, 2006); to be published as Yu. G. Naidyuk, O. E. Kvitnitskaya, I. K. Yanson, G. Fuchs, K. Nenkov, A. Wälte, G. Behr, D. Souptel, and S.-L. Drechsler, in Physica C (2007); doi:10.1016/j.physc.2007.03.165; see also cond-mat/0609770.
- [19] D. Souptel, G. Behr, W. Löser, K. Nenkov, G. Fuchs, J. of Crystal Growth, **275**, e91 (2005); D. Souptel, G. Behr, A. Kreyssig, W. Löser, J. of Crystal Growth, **276**, 652 (2005).
- [20] I.O. Kulik, A.N. Omel'yanchuk, R.I. Shekhter, Fiz. Nizk. Temp. **3**, 1543 (1977) [Sov. J. Low Temp. Phys. **3**, 740 (1977)]; I. O. Kulik, Fiz. Nizk. Temp. **18**, 450 (1992) [Sov. J. Low Temp. Phys. **18**, 302 (1992)].
- [21] A. Kreyssig, M. Loewenhaupt, J. Freudenberger, K.-H. Müller, and C. Ritter, J. Appl. Phys. **85**, 6058 (1999).
- [22] V.D. Fil, A. Knigavko, A.N. Zholobenko, E.-M. Choi, and S.-I. Lee, Phys. Rev. B **70**, 220504 (2004).
- [23] R. I. Shekhter and I.O. Kulik, Fiz. Nizk. Temp. **9**, 46 (1983) [Sov. J. Low Temp. Phys. **9**, 22 (1983)].
- [24] U. Gasser, P. Allenspach, F. Fauth, W. Henggeler, J. Mesot, A. Furrer, S. Rosenkranz, P. Vorderwisch, M. Buchgeister, Z. Phys. B **101**, 345 (1996);
- [25] N. Cavadini, Th. Strässle, P. Allenspach, P.C. Canfield, and Ph. Bourges, Eur. Phys. J B **29**, 377 (2002).
- [26] A. Kreyssig, O. Stockert, D. Reznik, F.M. Woodward, J.W. Lynn, H. Bitterlich, D. Souptel, G. Behr, M. Loewenhaupt, Physica C **408-410**, 100 (2004).
- [27] A. Kreyssig, O. Stockert, D. Reznik, F.M. Woodward, J.W. Lynn, W. Reichardt, D. Souptel, G. Behr, M. Loewenhaupt, Physica B **350** 69 (2004).
- [28] K.D.D. Rathnayaka, D.G. Naugle, B.K. Cho, P.C. Canfield, Phys. Rev. B **53**, 5688 (1996).
- [29] Yoshihiko Kobayashi, M. Iwata, T. Okamoto, H. Takeya, K. Kuroki, M. Suzuki and K. Asai, Physica B **378-380**, 475 (2006).
- [30] In discussing the value of  $\lambda_{PC}$  derived from a PC spectrum, we should always bear in mind that it is a transport coupling constant which in general differs from the

thermodynamic counter parts  $\lambda_s$ , although for some metals (see e.g. Ref. 9)  $\lambda_{PC} \approx \lambda_s$  holds accidentally.

- [31] M.B. Fontes, J.C. Trochez, B. Giordanengo, S.L. Budko, D.R. Sanchez, E.M. Baggio-Saitovitch, M.A. Continentino, *Phys. Rev. B* **60**, 6781 (1999).
- [32] B. I. Verkin, I. K. Yanson, I. O. Kulik, O. I. Shklyarevskii, A. A. Lysykh and Yu. G. Naidyuk, *Solid State Commun.*, **30** 215 (1979); *Izv. Akad. Nauk SSSR, Ser. Fiz.* **44** 1330 (1980).
- [33] I. O. Kulik, A. N. Omel'yanchuk, and I. K. Yanson, *Fiz. Nizk. Temp.* **7**, 263 (1981) [*Sov. J. Low Temp. Phys.* **7**, 129 (1981)].
- [34] Using equations for the conductivity of N-c-S contacts with magnetic impurities (see S.I. Beloborod'ko, *Low Temp. Phys.* **29**, 650 (2003)), calculations of the  $dV/dI$  curve display a smooth variation of the  $dV/dI$  shape (minimum) at the crossover to the gapless state (private communication by N. L. Bobrov). Thus, no abrupt suppression of the  $dV/dI$  gap minimum is expected by entering into the gapless state, contrary to our observation of  $dV/dI$  minima vanishing above  $T_N$ .
- [35] A. Amici, P. Thalmeier, and P. Fulde, *Phys. Rev. Lett.* **84**, 1800 (2000).
- [36] H. Doh, M. Sigrist, B.K. Cho, and S.-I. Lee, *Phys. Rev. Lett.* **83**, 5350 (1999) and H.-J. Kim, J.-H. Choi, H. Doh, E.-M. Choi, S.-I. Lee, M. Ohashi, and N. Mori, *Physica B* **327**, 438 (2003). In these papers a simple phenomenological Ginzburg-Landau model for the coexistence of magnetism and superconductivity in  $\text{Ho}_{1-x}\text{Dy}_x\text{Ni}_2\text{B}_2\text{C}$  has been proposed. Their "Ni derived" band corresponds to our isotropic FSS and their "non-Ni" derived band corresponds to our FSS's (which however do contain also Ni derived states!) where the magnetism quenches the superconductivity due to an admixture of Ho(Dy)  $5d$  states [5, 6]. Within this model below 4K far from the fluctuation region near 5K for  $\text{HoNi}_2\text{B}_2\text{C}$ , where the two magnetic phases still compete, the SC states of both compounds do almost coincide (see Fig. 3 of Ref. 36). This and the reported pressure dependencies are in qualitative accord with our microscopic picture leading to rather similar low-temperature SC states. However, we strongly differ in the description of the magnetically quenched band complex and its coupling to the "surviving" one. In our opinion, for the former the intrinsic el-ph phonon coupling is not weak but the interband coupling should be very weak by reasons of symmetry, at least in the pure unmixed limiting cases without a possible disorder induced locally broken symmetry. Only this way the well-known strong coupling properties of nonmagnetic borocarbides can be reproduced in switching off the magnetic couplings. Finally, we note that both scenarios should be distinguished from another phenomenological scenario proposed in Ref. 2 which is based on the assumption that the maximal reduction of the anisotropic spin-flip scattering achieved in the antiferromagnetically ordered state or equivalently  $T_N > T_c$  should be the necessary condition for the coexistence of local moment magnetism and superconductivity. A more detailed comparison and critical discussion of all three approaches will be given elsewhere.
- [37] A. I. Morozov, *Sov. Phys. Solid State* **22**, 1974 (1980); *JETP Lett.* **63**, 734 (1996).
- [38] B. T. Geilikman and V. Z. Kresin, *Sov. Physics Solid State*, **7**, 2659 (1966), *ibid.* **1**, 3294 (1965).
- [39] J. P. Carbotte, *Rev. Mod. Phys.* **62**, 1027 (1991).
- [40] S. V. Shulga and S.-L. Drechsler, *J. Low Temp. Phys.* (2001).
- [41] P. Fulde in "Handbook on the Physics and Chemistry of Rare Earths", K. Gscheidner and L.R. Eyring (Eds.) North-Holland Amsterdam, v. **2**, 295 (1978).
- [42] K. Winzer, K. Krug, and Z. Q. Peng, *J. of Mag. Magn. Mat.* **226-230**, 321 (2001).
- [43] I. K. Yanson, N. L. Bobrov, C. V. Tomy, and D. McK. Paul, *Physica C* **334** 33 (2000).
- [44] M. Diviš, K. Schwarz, P. Blaha, G. Hilscher, H. Michor, and S. Khmelevskiy, *Phys. Rev. B* **62**, 6774 (2000).
- [45] I. K. Yanson, in *Symmetry and Pairing in Superconductors* ed. by M. Ausloos and S. Kruchinin (Kluwer Academic Publisher, 1999) NATO Science Series II: Mathematics, Physics and Chemistry, Vol.63, p. 271.
- [46] H. Michor, M. El-Hagary, R. Hauser, E. Bauer, and G. Hilscher, *Physica B* **259**, 604 (1999).
- [47] I. K. Yanson, N. L. Bobrov, C. V. Tomy, and D. McK. Paul, *Physica C* **334** 152 (2000).
- [48] D. L. Bashlakov, Yu. G. Naidyuk, I. K. Yanson, G. Behr, S.-L. Drechsler, G. Fuchs, L. Schultz and D. Souptel, *J. Low Temp. Phys.* **147**, 335 (2007).
- [49] A. Wälte, unpublished.
- [50] S. N. Artemenko, A. F. Volkov and A. V. Zaitsev, *Solid State Commun.* **30**, 771 (1979).
- [51] S. I. Beloborod'ko, A. N. Omel'yanchuk, *Fiz. Nizk. Temp.* **17**, 994 (1991) [*Sov. J. Low Temp. Phys.* **17** 518 (1991)].
- [52] I. K. Yanson and Yu. G. Naidyuk, *Fiz. Nizk. Temp.* **30**, 355 (2004) [*Low Temp. Phys.* **30**, 261 (2004)]; Yu. G. Naidyuk, O. E. Kvitnitskaya, I. K. Yanson, S. Lee, and S. Tajima, *Solid State Commun.* **133**, 363 (2005).
- [53] D. L. Bashlakov, Yu. G. Naidyuk, I. K. Yanson, S. C. Wimbush, B. Holzapfel, G. Fuchs and S.-L. Drechsler, *Supercond. Sci. Technol.* **18**, 1094 (2005).